Thermodynamics of Bovine Spleen Galectin-1 Binding to Disaccharides: Correlation with Structure and Its Effect on Oligomerization at the Denaturation Temperature†

Frederick P. Schwarz,*,‡ Hafiz Ahmed,§ Mario A. Bianchet,|| L. Mario Amzel,|| and Gerardo R. Vasta§

Center for Advanced Research in Biotechnology and National Institute of Standards and Technology, 9600 Gudelsky Drive, Rockville, Maryland 20850, Center of Marine Biotechnology, University of Maryland Biotechnology Institute, Columbus Center, 701 East Pratt Street, Baltimore, Maryland 21202, and Department of Biophysics and Biophysical Chemistry, The Johns Hopkins University School of Medicine, 725 North Wolfe Street, Baltimore, Maryland 21205

Received July 8, 1997; Revised Manuscript Received October 15, 1997

ABSTRACT: Isothermal titration calorimetry (ITC) measurements of the binding 1-β carbohydrate-substituted galactopyranoside derivatives to galectin-1 from bovine spleen, a dimer with one binding site per subunit, were performed at 283−285 and 298 K. The disaccharides were lactose, methyl β-lactoside, lactulose, 4-*O*-β-D-galactopyranosyl-D-mannopyranoside, 3-*O*-β-D-galactopyranosyl-D-arabinose, 2′-*O*-methyllactose, lacto-*N*-biose, *N*-acetyllactosamine, and thiodigalactopyranoside. The site binding enthalpies, ΔH_b, are the same at both temperatures and range from -42.2 ± 3.3 kJ mol^{-1} for thiodigalactopyranoside to -24.5 ± 0.5 kJ mol^{-1} for lacto-*N*-biose, and the site binding constants range from $4.86 \pm 0.78 \times 10^3$ M^{-1} for methyl β-lactoside at 297.8 K to $6.54 \pm 0.97 \times 10^4$ M^{-1} for *N*-acetyllactosamine at 281.3 K. The binding reactions are enthalpically driven, exhibit enthalpy−entropy compensation, and, with the exception of *N*-acetyllactosamine, follow a van't Hoff dependence of the binding constant on temperature. The number of contacts at distances <4.0 Å between the disaccharide and galectin was determined from the energy-minimized conformation of the complex derived from the X-ray crystallographic structure of the galectin−*N*-acetyllactosamine complex determined by Liao et al. [Liao, D. I., Kapadia, G., Ahmed, H., Vasta, G. R., and Herzberg, O. (1994) *Proc. Natl. Acad. Sci. U.S.A. 91,* 1428−1432]. The binding enthalpies calculated from changes in the solvent-accessible surface areas of the galectin binding site upon binding of the disaccharide were in close agreement with the experimental values for lactose, lactulose, lacto-*N*-biose, and *N*-acetyllactosamine, all of which exhibit binding enthalpies >−36 kJ mol^{-1}. Differential scanning calorimetry measurements on solutions of galectin and its disaccharide complexes show that the galectin dimer does not dissociate upon denaturation in contrast to the legume lectins. At the denaturation temperature, the galectin in the absence of sugar exists as a tetramer, and the extent of this association is substantially reduced in the presence of a disaccharide.

Lectins bind to carbohydrates such as those on the surfaces of plant and animal cells with a high degree of specificity and effect processes within and without the cell. Although, over 5000 lectins have been isolated from biological systems, their precise biological functions are not yet fully understood. Information on the thermodynamics of their carbohydrate binding properties would help elucidate their biological roles. Previous investigations of the carbohydrate binding thermodynamics of plant lectins have shown that these reactions are enthalpically driven with little increase in the heat capacity change and they exhibit enthalpy−entropy compensation (*1*−*3*). Comparisons of the thermodynamics of binding of various carbohydrate derivatives to the X-ray crystallographic structure of a few of the carbohydrate−lectin complexes have successfully identified the structural determinants of the binding reactions (*4*). Recently, thermodynamic binding studies have been extended to lectins isolated from animal cells, specifically the galectins, to determine their thermodynamic binding properties. In particular, Ramkumar et al. (*5*) have shown that the carbohydrate binding reactions of the 14 kDa sheep spleen galectin are also enthalpically driven with little increase in the heat capacity change and they exhibit enthalpy−entropy compensation. If the structure of the carbohydrate−galectin complex were known, then comparison of the thermodynamics of the different carbohydrate derivatives would lead to the identification of the structural determinants such as the intermolecular interactions and changes in the solvent-accessible surface area responsible for the specificity of the binding thermodynamics. This knowledge is important in elucidating the relationship between structure and function in lectins, as well as the specific biological role of the galectins.

† Supported by Grant 03-4-38512 from the Collaborative Research Program, University of Maryland Biotechnology Institute, to F.P.S. and G.R.V., Grant 95-31 from the Lucille P. Markey Trust Fund, and Grant MCB-94-06649 from the National Science Foundation to G.R.V.

* To whom correspondence should be sent.

‡ Center for Advanced Research in Biotechnology and National Institute of Standards and Technology.

§ University of Maryland Biotechnology Institute.

|| The Johns Hopkins University School of Medicine.

S0006-2960(97)01647-4 CCC: $15.00
Published on Web 04/14/1998

Galectins are S-type β-galactosyl-binding lectins that are calcium-independent and require a reducing environment for their binding activity (*6*−*8*). Binding inhibition studies have suggested that 4′-OH and 6′-OH of the galactopyranosyl ring and the 3-OH of the glucopyranoside ring in lactose and the lactosaminoglycans are primarily responsible for interactions with galectin (*9*−*11*). The crystal structure of the bovine spleen galectin complexed with *N*-acetyllactosamine, determined recently to 1.9 Å resolution (*12*), confirmed the above interactions with possible hydrogen bonding of the 4′-OH with His44 and Arg48, 6′-OH with Asn61, and 3-OH of the *N*-acetylglucopyranoside ring with Arg48, Glu71, and Arg73. Additional possible hydrogen-bonding interactions involving water were predicted between His52, Asp54, and Arg73 and the nitrogen of the *N*-acetyl group on the C-2 of the glucopyranoside ring. Comparison of the binding thermodynamics of disaccharides with different substituents on the glucopyranoside ring then can confirm these interactions, particularly if the thermodynamic binding quantities correlate with the number of close contacts between the disaccharide and the galectin or with changes in the solvent-accessible surface area of the galectin binding site. Although two galectin monomer units combine to form a dimer with a topology similar to that of the legume lectins, the ligand binding site is topologically different from that of the legume lectins and consists of a unique set of salt bridges (*12*).

In this investigation, isothermal titration calorimetry (ITC)[1] was employed to determine the thermodynamics of the disaccharide−galectin binding reaction in terms of the site binding constant (K_b) and changes in the free energy (ΔG_b°), the binding enthalpy (ΔH_b), and the binding entropy (ΔS_b). The binding reaction between the galectin binding site and the disaccharide ligand (L) is

$$\text{galectin} + \text{L} \leftrightarrow \text{galectin}\cdot\text{L} \qquad (1)$$

in 0.15 M NaCl + 0.02 M sodium phosphate buffer at pH = 7.4 (PBS) containing 2 mM DTT reducing reagent. The titration calorimetry measurements were performed around 285 and 297 K with a series of 1-β carbohydrate-substituted galactopyranoside derivatives very similar in structure to *N*-acetyllactosamine (Galβ1,4GlcNAc). Basically, the disaccharides consisted of derivatives where the nonreducing Gal moiety, with the exception of 2′-*O*-methyllactose, is the same so that the intermolecular interactions can be compared for only the subterminal monosaccharide unit of each disaccharide. Although each of the subterminal monosaccharide units differs in the distribution of OH groups and OH-substituted groups, the pyranoside ring of the subterminal unit has the $^1C_4$ (chair form) conformation as the lowest energy conformation in the unligated state (*13*, *14*). These derivatives consisted of lactose (Galβ1,4Glc), 4-*O*-β-D-galactopyranosyl-D-mannopyranoside (Galβ1,4Man), 3-*O*-β-D-galactopyranosyl-D-arabinose (Galβ1,3Ara), thiodigalactopyranoside (Galβ1S1βGal), methyl β-lactoside (Galβ1,4Glcβ-OMe), lactulose (Galβ1,4Fruc), and lacto-*N*-biose (Galβ1,3GlcNAc).

Two approaches were utilized to relate the specificity of the binding thermodynamics to the structural determinants of the disaccharide−galectin complex. The energy-minimized structures were derived from the crystal structure of the Galβ1,4GlcNAc−galectin complex (*12*) with suitable substitutions on the glucopyranoside moiety, e.g., with OH replacing the NHAc group on C-2 for the starting structure of Galβ1,4Glc. The simpler approach was to correlate the number of atoms on the disaccharide within 4.0 Å of the atoms of the amino acid residues at the galectin binding site to the binding enthalpy, i.e., the number of close contacts, on the assumption that the greater the number of contacts, the more negative the binding enthalpy. The second approach compared the experimental binding enthalpies to those calculated from changes in the solvent-accessible surface area of the galectin binding site upon binding of the disaccharide (*15*). The thermodynamic binding quantities for Galβ1,4Glcβ-OMe and 2′-*O*-methyllactose (MeO-2Galβ1,4Glc) were determined to evaluate the effect of a substituent on the binding thermodynamics.

In addition, the effect of disaccharide binding on the structural stability of galectin was investigated by differential scanning calorimetry (DSC) and compared to previous studies on the unfolding of the topologically similar dimer concanavalin A. Although concanavalin A exists as a tetramer at the denaturation temperature and dissociates into monomers upon thermal denaturation (*2*), it will be shown that galectin likewise exits as a tetramer but does not dissociate upon unfolding.

EXPERIMENTAL PROCEDURES

Materials. The galectin was prepared from bovine spleen on a lactosyl-Sepharose[2] column following the improved purification protocol as described by Ahmed et al. (*16*). Briefly, the spleen extract in 10-fold diluted PBS containing 0.01 M 2-mercaptoethanol (ME) and 0.1 M lactose at pH 7.5 was absorbed on DEAE-Sepharose and washed with PBS (diluted 10-fold) containing 0.01 M ME to remove the lactose, and then the bound protein was eluted with PBS containing 0.01 M ME, 0.002 M EDTA, and 0.5 M NaCl. The high salt eluate was then absorbed on a lactosyl-Sepharose column preequilibrated with PBS + 0.01 M ME + 0.002 M EDTA + 0.5 M NaCl column buffer. After the column was washed with the column buffer followed by 10-fold diluted PBS containing ME, the bound protein was eluted with 10-fold diluted PBS + 0.01 M ME + 0.1 M lactose solution and stored on several DEAE-Sepharose columns (0.5 mL bed volume) overlaid with 50% glycerol in eluting buffer at −20 °C until needed. The purity of the galectin was assessed by SDS−PAGE on 15% polyacrylamide gel in the presence of ME and by gel permeation chromatography on Superose 6 column from Pharmacia. The

[1] Abbreviations: DSC, differential scanning calorimetry; ITC, isothermal titration calorimetry; ME, 2-mercaptoethanol; PBS, 0.02 M sodium phosphate buffer containing 0.15 M NaCl at pH = 7.4; DTT, dithiothreitol; Galβ1,4Glc, lactose; Galβ1,4Man, 4-*O*-β-D-galactopyranosyl-D-mannopyranoside; Galβ1,3Ara, 3-*O*-β-D-galactopyranosyl-D-arabinose; Galβ1S1βGal, thiodigalactopyranoside; Galβ1,4Glcβ-OMe, methyl β-lactoside; Galβ1,4Fruc, lactulose; Galβ1,3GlcNAc, lacto-*N*-biose; Galβ1,4GlcNAc, *N*-acetyllactosamine; MeO-2Galβ1,4Glc, 2′-*O*-methyllactose.

[2] Certain commercial equipment, instruments, and materials are identified in this paper in order to specify the experimental procedure as completely as possible. In no case does this identification imply a recommendation or endorsement by the National Institute of Standards and Technology, nor does it imply that the material, instrument, or equipment identified is necessarily the best available for the purpose.

specific activity of the purified galectin was checked by the agglutination with rabbit protease treated erythrocytes (*16*).

The disaccharides were the highest purity available from Sigma Chemical Co. and used without further purification.

Preparation and Analysis of Solutions. The DEAE-Sepharose column containing galectin was washed with 10-fold diluted PBS containing 0.01 M ME to remove glycerol and lactose, eluted with 2 mL of PBS + 0.01 M ME + 0.5 M NaCl. The elutant solution was then extensively dialyzed in PBS containing 2 mM dithiothreitol (DTT). The concentrations of the protein solutions were determined from UV spectroscopic measurements at 280 nm where the 1 cm absorbance of a 1 mg mL^{-1} galectin solution is 0.65 (*16*).

Solutions of the carbohydrates were prepared by weight in the dialysate to minimize differences between the protein buffer solution and ligand buffer solution in the ITC measurements. Milligram quantities of the sugar were added directly to 0.5 g of the galectin solution in the DSC cell for the DSC measurements.

ITC Measurements and Analysis. The ITC measurements were performed with a Microcal Omega titration calorimeter as described previously by Wiseman et al. (*17*) and Schwarz et al. (*2*). Aliquots of the ligand solution at 10−20 times the site concentration were added via a 100 μL rotating stirrer−syringe to the solution cell containing 1.385 mL of the 0.02−0.05 mM protein (dimer) solution. The heat of dilution was determined to be negligible in separate titrations of the ligand solution into just the buffer solution.

An identical site model, utilizing a site concentration = 2[galectin] (2[G]), was the simplest binding model found to provide the best fit to the ITC data. The total heat content, Q_t, is related to the total disaccharide concentration, $[L]_t$, via the equation (*17*):

$$Q_t = 2n[G]_t\Delta H_b V\{1 + [L]_t/2n[G]_t + 1/2nK_b[G]_t - [(1 + [L]_t/2n[G]_t + 1/2nK_b[G]_t)^2 - 4[L]_t/2n[G]_t]^{1/2}\}/2 \quad (2)$$

where n is the stoichiometry and V is the cell volume. The expression for the heat released per the ith injection, $\Delta Q(i)$, is then (*18*)

$$\Delta Q(i) = \Delta Q(i) + dV_i/2V[Q(i) + Q(i-1)] - Q(i-1) \quad (3)$$

where dV_i is the volume of titrant added to the solution.

The thermodynamic quantities, ΔG_b° and ΔS_b, were obtained from the basic equation of thermodynamics

$$\Delta G_b^\circ = \Delta H_b - T\Delta S_b \quad (4a)$$

where

$$\Delta G_b^\circ = -nRT\ln\{K_b\} \quad (4b)$$

and n = number of moles, T is the absolute temperature, and $R = 8.3151$ J mol^{-1} K^{-1}.

Energy-Minimized Conformations of the Disaccharide−Galectin Complex. Molecular conformations of the disaccharide in the binding site were obtained using Quanta version 4.1 (*19*) and the X-ray crystallographic structure of the Galβ1,4GlcNAc−galectin complex (*12*) as the starting structure with the suitable substitutions on the glucopyranoside moiety. The overlapping nonreducing galactopyranoside common to all the disaccharides was maintained in the conformation observed in the X-ray crystallographic structure. Substitutions and different epimerizations of the second moiety were regularized and minimized using the program CHARMm version 2.3 while constraining the changes to the first coordination sphere of the atoms affected by the change. Starting conformations of the glucopyranoside moiety were in the chair form as indicated in the X-ray structure and in refs *13* and *14*. In cases for which the substituted group had one or more degrees of freedom, conformational searches were performed and the conformations at the energy minima were used. For Galβ1S1βGal, the molecule observed in the bufo lectin−Galβ1S1βGal complex (*20*) was used with its nonreducing end aligned with the nonreducing end of Galβ1,4GlcNAc in the Galβ1,-4GlcNAc−galectin complex. Interatomic distances between the amino acid residues at the binding site and the carbohydrate moiety of less than 4.0 Å were then identified as possible hydrogen-bonding interactions. The interatomic distances for the Galβ1,4GlcNAc−galectin complex were taken directly from the X-ray structure in the Brookhaven Protein Data Bank (file 1SLT.dpb).

Calculation of Binding Enthalpies. The binding enthalpies were calculated using the following equations where the changes in the solvent-accessible surface areas at the binding site upon binding, ΔASA, are as described in detail by Luque et al. (*15*). The binding enthalpies are related to ΔASA as follows:

$$\Delta H_b(T) = \Delta H_b(T_R) + \int^T \Delta C_p(T)\, dT \quad (5)$$

with

$$\Delta H_b(T_R) = a_H(T_R)\Delta\text{ASA}_{\text{apolar}} + b_H(T_R)\Delta\text{ASA}_{\text{polar}} \quad (5a)$$

$$\Delta C_p(T) = \Delta C_{p,\text{apolar}}(T) + \Delta C_{p,\text{polar}}(T) \quad (5b)$$

where

$$T_R = 333 \text{ K}$$

and

$$\Delta C_p(T) = a_C(T)\Delta\text{ASA}_{\text{apolar}} + b_C(T)\Delta\text{ASA}_{\text{polar}} + c_C\Delta\text{ASA}_{\text{OH}} \quad (5c)$$

where

$$a_H(T_R) = -35.32 \text{ J mol}^{-1} \text{ Å}^{-2} \quad (5d)$$

$$b_H(T_R) = 131.4 \text{ J mol}^{-1} \text{ Å}^{-2} \quad (5e)$$

$$a_C(T) = 1.88 + (1.10 \times 10^{-3})(T - 298.2 \text{ K}) - (1.76 \times 10^{-4})(T - 298.2 \text{ K})^2 \text{ at } 298.2 \text{ K} \quad (5f)$$

$$b_C(T) = -1.09 + (1.19 \times 10^{-3})(T - 298.2 \text{ K}) - (1.80 \times 10^{-4})(T - 298.2 \text{ K})^2 \text{ at } 298.2 \text{ K} \quad (5g)$$

and

$$c_C = 0.71 \text{ J mol}^{-1} \text{ Å}^{-2} \text{ at } 298.2 \text{ K} \quad (5h)$$

Although these coefficients were derived from correlating changes in the heat capacity and enthalpy upon unfolding of a protein in solution to the change in its solvent-accessible surface area, this treatment has been applied successfully toward predicting the energetics of angiotensin II binding to its antibody from the crystal structure of the complex (*21*). Differences in the solvent-accessible surface areas were calculated using the software programs AREAIMAL, DIFFAREA, and SURFACE in the CCP4 suite of programs (*22*). These programs find solvent-accessible areas of atoms in a Brookhaven coordinate file using the Lee and Richards algorithm (*23*). The probe radius was 1.4 Å and the slice was 0.25 Å.

DSC Measurements and Analysis. DSC measurements were performed with a Hart 7707 DSC heat conduction scanning microcalorimeter which consists of three removable 1 mL solution cells and a reference cell. The measurements were usually performed at a scan rate of 15 K h^{-1}. To determine any dependence of the parameters on scan rate, scans were also performed at 25 K h^{-1}. Least-squares fit of the two-state transition model, A ↔ B, where A is the folded state and B is the unfolded state, to the data was performed by the EXAM program (*24*). This program utilizes a sigmoidal baseline and the ΔC_p for the transition to yield a van't Hoff enthalpy (ΔH_v), a transition temperature (T_m, the temperature at half the peak area), and the transition peak area which when divided by the number of moles of protein in the cell yields the calorimetric enthalpy (ΔH_c). The ratio of $\Delta H_c/\Delta H_v$ indicates the size of the molecular galectin unit participating in the transition; e.g., a ratio of <1.0 indicates that more than one galectin dimer is participating in the transition. The EXAM program has the option of correcting the DSC scans for the 138 s response time of the DSC via the Tian equation. However, this correction to the scans performed at 15 K h^{-1} not only introduced additional noise in the resulting DSC scans but also resulted in changes in T_m, ΔH_c, and ΔH_v well within their experimental errors. Thus, the DSC scans at this slower scan rate were not corrected for the time response of the DSC. Application of the Tian equation to the scans performed at 25 K h^{-1} did produce changes in T_m and ΔH_v greater than their experimental errors, and thus, these faster DSC scans were corrected for the slow response time of the DSC. The determination of the binding constant at the denaturation temperature from the DSC measurements has been described previously (*25*). More specifically, the binding constant is determined from the increase in the denaturation temperature in the presence of the ligand (T_l), the calorimetric enthalpy of the dimer, and the concentration of the ligand, as shown by the equation:

$$K_b(T_l) = [\exp\{(T_l - T_m)\Delta H_c(T_l)/2.0RT_lT_m\} - 1]/[L] \quad (6)$$

RESULTS

The galectin preparations for all ITC and DSC measurements were consistent with results published elsewhere (*16*) with respect to their purity and mobility on SDS−PAGE, where the protein yields a single band corresponding to 14.5 kDa, a retention time on FPLC gel permeation chromatography where the protein yields a single peak corresponding to 28.5 kDa, and the specific activity of $1.7-2.0 \times 10^4$ mL mg^{-1}. The storage of the purified galectin on the DEAE-Sepharose column with 50% glycerol in the eluting buffer for long periods of time at 253 K ensured the full activity of the protein by preventing oxidation and denaturation that normally occur in solution.

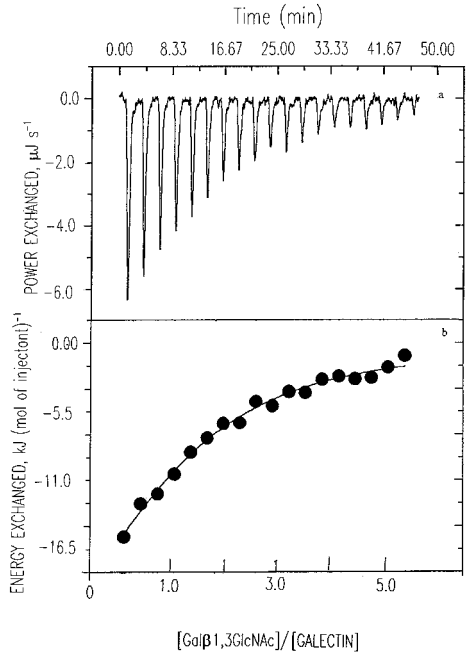

FIGURE 1: (a) Titration calorimeter results from addition of 5 μL aliquots of 2.26 mM Galβ1,3GlcNAc in PBS + 2 mM DTT to 0.027 mM galectin in PBS + 2 mM DTT at 280.9 K. (b) Plot of the total heat released as a function of total ligand concentration for the titration shown in panel a. The solid line is the result of the best least-squares fit of the data to eq 3.

Results of a typical titration calorimetry measurement, which consisted of adding 5 μL aliquots of 2.26 mM Galβ1,-3GlcNAc in PBS + 2mM DTT to 0.027 mM galectin in PBS + 2 mM DTT (1.385 mL) at 280.9 K, are shown in Figure 1. A least-squares fit of the ITC data to the identical site model described by eq 3 is also presented in Figure 1. The close fit of the data to the identical site model shows that the ligand binds to each of the two binding sites of galectin independently and with the same binding constant and enthalpy. The results of the disaccharide titrations are presented in Table 1 and show that the binding reactions are essentially enthalpically driven with little dependence of the enthalpy on temperature from 280 to 300 K. Values for ΔH_b range from −42.2 kJ mol^{-1} for Galβ1S1βGal to −24.5 kJ mol^{-1} for Galβ1,3GlcNAc. Values for K_b range from $0.486 \pm 0.076 \times 10^4$ M^{-1} for Galβ1,4Glcβ-OMe at 297.8 K to $6.54 \pm 0.97 \times 10^4$ M^{-1} for Galβ1,4GlcNAc at 281.3 K and agree on a relative basis with the values determined by an independent inhibition method (*16*) (Table 2). The relative binding affinities for those disaccharides with the bovine spleen galectin-1 are comparable with the values for most galectins-1 (*9*−*11*) or galectins with conserved CRDs (*26*, *27*). The calculated values of the binding enthalpy from the van't Hoff equation

$$\ln\{K_b(T)/K_b(T_0)\} = -\Delta H_v[1/T_0 - 1/T]/R \quad (7)$$

are in good agreement with the ITC binding enthalpies as also shown in Table 1. The largest discrepancy between the calculated van't Hoff enthalpy and the ITC value is for

Table 1: Thermodynamic Quantities on the Binding of Disaccharide Derivatives to Galectin in PBS Buffer Containing 2.0 mM DTT at pH = 7.4[a]

	T (°C)	K_b ($\times 10^4$ M^{-1})	$\Delta G_b°$	ΔH_b (kJ mol^{-1})	$T\Delta S_b$	ΔS_b (J mol^{-1} K^{-1})
Galβ1,4Glc	297.1	0.644 ± 0.092	−21.7 ± 0.4	−20.9 ± 1.8	0.8 ± 1.8	0
	296.3	0.655 ± 0.050	−21.6 ± 0.2	−26.8 ± 0.9	−5.2 ± 0.9	−18 ± 3
	284.8	1.00 ± 0.05	−21.8 ± 0.1	−25.6 ± 0.6	−3.8 ± 0.6	−13 ± 2
	285.1	0.93 ± 0	−21.6 ± 0.1	−28.3 ± 0.6	−6.7 ± 0.6	−24 ± 2
	ΔH_v[a] = −22.4 ± 2.9 kJ mol^{-1} ave values			−25.4 ± 3.2		−18 ± 7
Galβ1,4Glcβ-OMe	297.8	0.486 ± 0.076	−21.0 ± 0.4	−29.5 ± 3.0	−8.5 ± 3.0	−29 ± 10
	288.9*	0.591 ± 0.052	−21.4 ± 0.2	−27.0 ± 1.5	−5.6 ± 1.5	−19 ± 5
	283.3	0.866 ± 0.051	−21.3 ± 0.1	−25.4 ± 0.7	−4.1 ± 0.7	−14 ± 2
	281.8	0.899 ± 0.038	−21.3 ± 0.9	−31.5 ± 0.7	−10.2 ± 1.1	−36 ± 4
	ΔH_v[a] = −27.1 ± 0.6 kJ mol^{-1} ave values			−28.4 ± 2.7		−25 ± 10
Galβ1,4Fruc	298.5	0.82 ± 0.10	−22.4 ± 0.3	−34.4 ± 2.7	−12.0 ± 2.7	−40 ± 9
	297.3	1.08 ± 0.12	−23.0 ± 0.3	−26.6 ± 1.6	−3.6 ± 1.6	−12 ± 5
	282.9	1.87 ± 0.13	−23.2 ± 0.2	−28.2 ± 0.7	−5.0 ± 0.7	−18 ± 2
	281.2	2.13 ± 0.12	−23.3 ± 0.1	−34.4 ± 0.8	−11.1 ± 0.8	−39 ± 3
	ΔH_v[a] = −33.6 ± 4.9 kJ mol^{-1} ave values			−30.3 ± 4.1		−27 ± 14
Galβ1,4Man	296.3	1.13 ± 0.12	−23.0 ± 0.3	−35.2 ± 2.1	−13.2 ± 2.1	−45 ± 7
	295.8	0.86 ± 0.07	−22.9 ± 0.2	−39.3 ± 1.7	−16.4 ± 1.7	−55 ± 6
	284.2	1.85 ± 0.15	−23.2 ± 0.2	−36.0 ± 1.3	−12.8 ± 1.3	−45 ± 5
	284.2	1.94 ± 0.11	−23.3 ± 0.1	−33.5 ± 0.8	−10.2 ± 0.8	−36 ± 3
	ΔH_v[a] = −38.2 ± 4.5 kJ mol^{-1} ave values			−36.0 ± 2.4		−45 ± 8
Galβ1,3Ara	298.1	0.54 ± 0.07	−21.3 ± 0.3	−36.8 ± 2.5	−15.5 ± 2.5	−52 ± 8
	296.1	0.75 ± 0.06	−22.0 ± 0.2	−44.8 ± 1.7	−22.8 ± 1.7	−77 ± 6
	283.1	1.84 ± 0.12	−23.1 ± 0.2	−45.2 ± 1.2	−22.1 ± 1.2	−78 ± 3
	280.8	1.92 ± 0.20	−23.0 ± 0.2	−34.4 ± 2.8	−11.4 ± 2.8	−41 ± 10
	ΔH_v[a] = −49.8 ± 5.3 kJ mol^{-1} ave values			−40.3 ± 5.5		−62 ± 18
Galβ1,3GlcNAc	296.8	1.67 ± 0.16	−24.0 ± 0.2	−29.5 ± 1.4	−5.5 ± 1.4	−19 ± 5
	296.2	2.09 ± 0.18	−24.5 ± 0.2	−24.2 ± 0.9	0.3 ± 0.9	0
	281.3	3.00 ± 0.27	−24.1 ± 0.2	−25.1 ± 0.9	−1.0 ± 0.9	0
	280.9	3.80 ± 0.40	−24.6 ± 0.3	−24.3 ± 0.8	0.3 ± 0.8	0
	ΔH_v[a] = −26.9 ± 6.7 kJ mol^{-1} ave values			−25.7 ± 2.5		0
MeO-2Galβ1,4Glc	297.7	1.95 ± 0.20	− 24.4 ± 0.2	−30.6 ± 1.9	−6.2 ± 1.9	−19 ± 6
	297.0	2.06 ± 0.15	−24.5 ± 0.2	−31.7 ± 1.1	−7.2 ± 1.1	−24 ± 4
	283.2	4.25 ± 0.53	−25.1 ± 0.3	−26.6 ± 1.3	−1.5 ± 1.3	0
	281.7	4.07 ± 0.25	−24.9 ± 0.1	−31.5 ± 0.6	−6.6 ± 0.6	−23 ± 2
	ΔH_v[a] = −33.9 ± 2.9 kJ mol^{-1} ave values			−30.1 ± 2.4		−22 ± 3
Galβ1,4GlcNAc	298.2*	1.01 ± 0.79	−22.9 ± 1.9	−32.5 ± 5.4	−9.6 ± 5.7	−32 ± 19
	296.8	2.22 ± 0.96	−24.7 ± 1.1	−35.9 ± 0.7	−11.2 ± 1.3	−38 ± 4
	281.3	6.54 ± 0.97	−25.9 ± 0.3	−30.3 ± 1.0	−4.4 ± 1.0	−16 ± 4
	280.2	5.58 ± 0.99	−25.5 ± 0.4	−29.8 ± 1.9	−4.3 ± 1.9	−15 ± 7
	ΔH_v[a] = −42.7 ± 8.6 kJ mol^{-1} ave values			−30.9 ± 1.4		−25 ± 9
Galβ1S1βGal	297.0	1.16 ± 0.24	−23.1 ± 0.5	−46.4 ± 7.4	−23.3 ± 7.4	−78 ± 25
	296.1	1.98 ± 0.17	−24.4 ± 0.2	−43.1 ± 1.8	−18.7 ± 1.8	−63 ± 6
	280.2	4.26 ± 0.57	−24.8 ± 0.3	−38.1 ± 1.3	−17.3 ± 1.3	−62 ± 5
	280.0	6.21 ± 0.94	−25.7 ± 0.4	−40.2 ± 4.5	−14.5 ± 4.5	−52 ± 16
	ΔH_v[a] = −41.3 ± 13.6 kJ mol^{-1} ave values			−42.2 ± 3.3		−64 ± 11

[a] ΔH_v values were calculated from a van't Hoff plot of K_b vs 1/T(K) and K_b* values were deleted from the van't Hoff plot. The errors are the standard deviations of at least two determinations of the binding quantities.

Galβ1,4GlcNAc, which is lower by 12 ± 9 kJ mol^{-1} than the ITC binding enthalpy. The binding reactions also exhibit enthalpy−entropy compensation as shown in Figure 2.

The energy-minimized conformations of the complexes determined from the Galβ1,4GlcNAc−galectin crystal structure and the low-energy conformations of the disaccharides (Figure 3) are shown in Figure 4. The close contacts identifiable as atoms of the binding site within 4.0 Å of atoms on the carbohydrate are presented in Table 3. Using this criterion, the close contacts between the glucopyranoside-substituted moiety and the galectin binding site are between OH groups on the glucopyranoside and the nitrogen atoms of Arg48 and Arg73, the oxygen atoms of Glu71, and the atoms of bridging water molecules between the OH groups and the amino acid residues as shown in Figure 4. The comparison between the number of close contacts and

Table 2: Comparison of Results for Inhibition of Galectin Binding to Asialofetuin and ITC Determined Binding Constants at 298.2 K

ligand	relative activity from inhibition[a]	relative ITC K_b[b]
Galβ1,4Glc	1	1.2 ± 0.2
Galβ1,4Glcβ-OMe	1.3	1.2 ± 0.1
Galβ1,4Fruc	1.9	2.2 ± 0.2
Galβ1,4Man	2.3	1.7 ± 0.1
Galβ1,3Ara	2.6	1.5 ± 0.1
Galβ1,3GlcNAc	4.0	4.2 ± 0.4
MeO-2Galβ1,4Glc	4.1	4.1 ± 0.3
Galβ1,4GlcNAc	5.5	4.4 ± 2.0
Galβ1S1βGal	5.9	4.0 ± 0.3

[a] Values were taken from ref *16*. [b] The relative K_b values are based on assigning a value of 4.1 to the MeO-2Galβ1,4Glc binding constant. The errors are the standard deviations of at least two determinations of the binding constants.

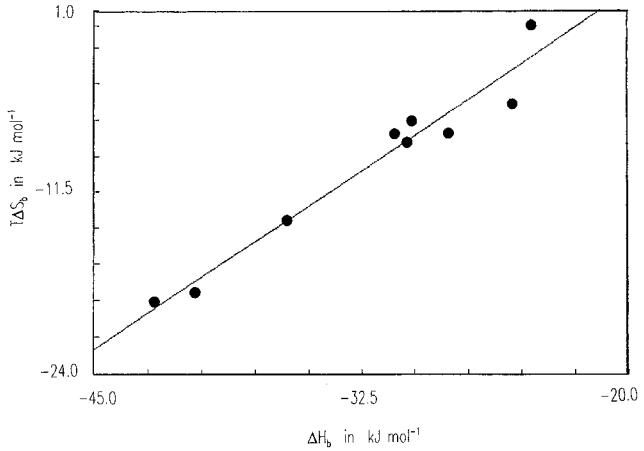

FIGURE 2: Plot of $T\Delta S_b$ versus ΔH_b for the binding of carbohydrates to galectin at 298.2 K. The line is the best least-squares fit of the data to a straight line and is described by $T\Delta S_b$ (kJ mol^{-1}) = (21.9 ± 2.7) × 10^3 + (0.98 ± 0.08)ΔH_b (kJ mol^{-1}).

binding enthalpies summarized in Table 4 shows that there is no correlation between this thermodynamic quantity and the number of close contacts. Further reduction in the close contact distance to, for example, distances less than 3.5 Å between the carbohydrate groups and the galectin binding site would reduce the number of close contacts for Galβ1S1βGal, as shown in Table 3, from 7 to 6, which again showed a lack of correlation between the number of close contacts and the binding enthalpies.

The binding enthalpies calculated from differences in the solvent-accessible surface areas at the binding site are presented in Table 4. The calculated binding enthalpies are all in the range −27.6 to −23.5 kJ mol^{-1} and are within two standard deviations of the binding enthalpies of Galβ1,-3GlcNAc, Galβ1,4Glc, Galβ1,4Fruc, and Galβ1,4GlcNAc.

A typical DSC scan of galectin in PBS + 2 mM DTT is shown in Figure 5 along with the fit of the single transition peak data to the A = B two-state transition model. The transition peak did not reappear upon a rescan of the sample, indicating that the transition is irreversible. Although a slightly better fit was obtained with a A_2 = 2B two-state dissociative transition model in a few DSC scans, T_m does not exhibit the 2 K increase expected from a 0.043 to 0.179 mM increase in the galectin concentration (1) from this model. Thus, application of this model to the results is not justified. Results of the fit of the transition peak data to the two-state transition model are presented in Table 5. At the higher DSC scan rate, T_m, ΔH_v, and ΔH_c are within experimental error of their values determined at the slower scan. Since T_m , ΔH_v, and ΔH_c at the different scan rates are the same, the equilibrium two-state transition model was applied to these transitions instead of the irreversible model of Sanchez-Ruiz (*28*). This analysis of the irreversible galectin transitions in terms of a thermodynamic model is based on treating the transitions as a sequence of two processes: the reversible unfolding of the protein described by the unfolding temperature and the calorimetric enthalpy followed by a slower irreversible process such as aggregation. This approach yields results for the overall process that are the same as for the reversible process (*29*). In Table 5, the ratio of $\Delta H_c/\Delta H_v$ is 0.25, which is indicative of galectin existing as a tetramer at the denaturation temperature. Since

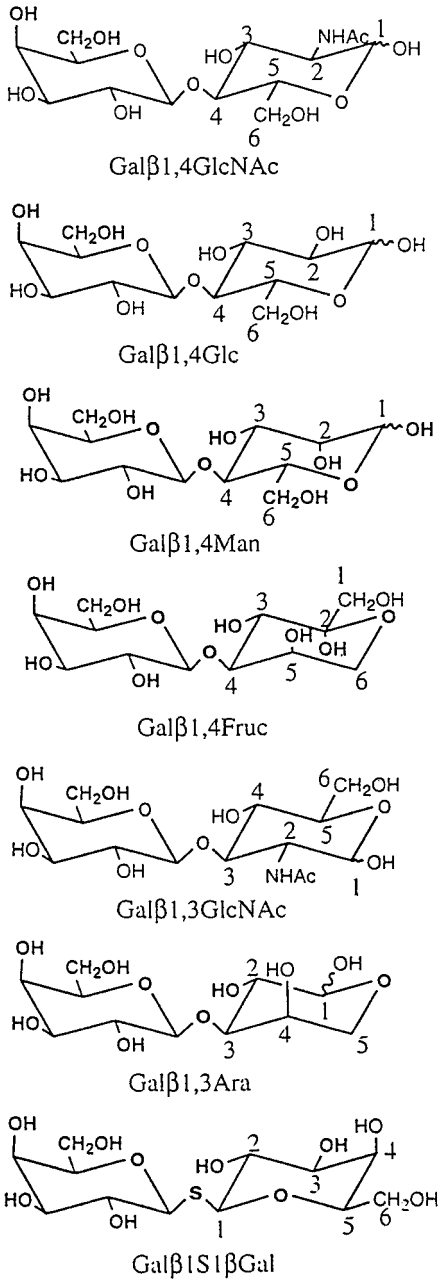

FIGURE 3: Lowest energy conformations of the disaccharides from refs *13* and *14*.

galectin does not dissociate upon denaturation, galectin maintains this association in the unfolded state. There is a slight, 1 K, increase in the denaturation temperature with a decrease in pH from 7.6 to 6.8, indicating a slightly higher stability of the protein at the lower pH.

DSC scans of galectin in the presence of saturating amounts of carbohydrate ligands exhibit a single transition which is again best fitted to a A = B two-state transition model as shown in Figure 5. The results of fitting the model to the DSC data for the unfolding of galectin in the presence of Galβ1,4Glc, Galβ1,4Man, MeO-2Galβ1,4Glc, and Gal-β1S1βGal are presented in Table 6. T_l increases with ligand concentration while values for ΔH_v remain the same. Values for ΔH_c are almost doubled in the presence of ligand, as shown in Figure 5 by the large increase in the area of the higher temperature transition peak, so that the ratio $\Delta H_c/\Delta H_v$ is between 0.5 and 1.00. This implies that when

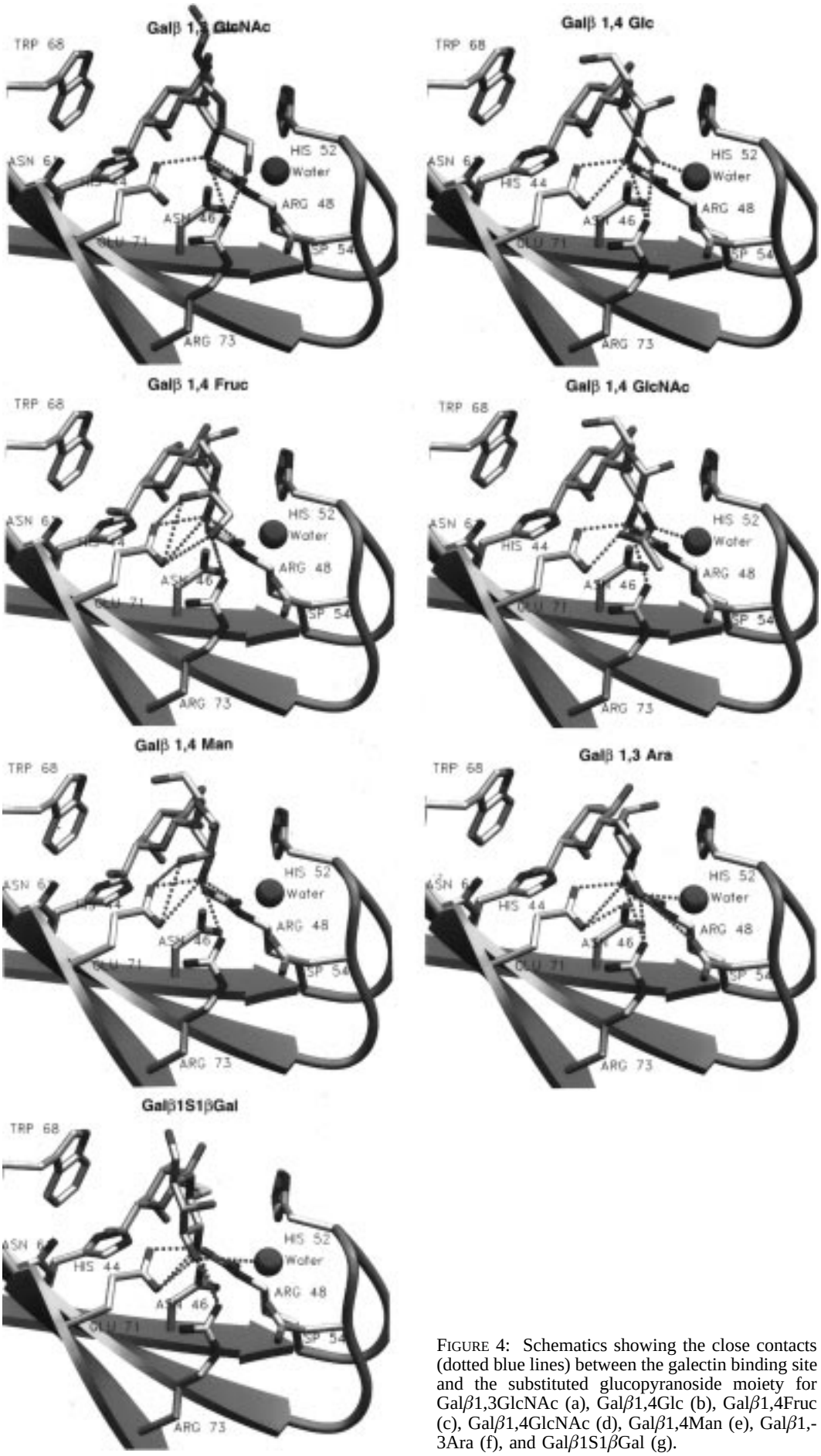

FIGURE 4: Schematics showing the close contacts (dotted blue lines) between the galectin binding site and the substituted glucopyranoside moiety for Galβ1,3GlcNAc (a), Galβ1,4Glc (b), Galβ1,4Fruc (c), Galβ1,4GlcNAc (d), Galβ1,4Man (e), Galβ1,-3Ara (f), and Galβ1S1βGal (g).

Table 3: Contacts at Distances <4.0 Å between the Subterminal Monosaccharide of Each Disaccharide and Galectin from Molecular Dynamics Simulations

disaccharide [$-\Delta H°_b$ (kJ mol^{-1})]	subterminal monosaccharide group	distances to protein atoms (Å)					
		N_η1 Arg48	N_η2 Arg48	O_e1 Glu71	O_e2 Glu71	N_η2 Arg73	H_2O
Galβ1,3GlcNAc	4-OH	2.75	3.23		2.44	3.27	
(24.5 ± 0.5)	6-OH					2.49	
Galβ1,4Glc	2-OH					3.37	2.49
(25.4 ± 3.2)	3-OH	2.75	3.23	3.34	2.44	3.27	
Galβ1,4Fruc	1-OH					2.36	2.01
(30.3 ± 4.1)	2-OH			3.39	2.75		
	3-OH	2.73	3.21		2.42	3.38	
	5-OH			3.20		2.94	
Galβ1,4GlcNAc	2-N			4.00			2.64
(30.9 ± 1.4)	3-OH	2.75	3.23	3.34	2.44	3.27	
Galβ1,4Man	2-OH			3.39	2.86		
(36.0 ± 2.4)	3-OH	2.75	3.23	3.34	2.44	3.27	
Galβ1,3Ara	1-OH			3.26		2.54	2.64
(40.3 ± 3.3)	2-OH	2.54		3.44	2.43	3.40	
Galβ1S1βGal	1-S	3.98					
(42.2 ± 3.3)	2-OH	2.94		3.01	2.23	3.09	
	3-OH			2.87		3.16	3.80

Table 4: Comparison of Experimental to Calculated Binding Enthalpies for Binding of the Disaccharides to Galectin

disaccharide	no. of close contacts at distances <4.0 Å	$-$exptl ΔH_b (kJ mol^{-1})	$-$calcd ΔH_b[a] (kJ mol^{-1})
Galβ1,3GlcNAc	5	24.5 ± 0.5	27.6
Galβ1,4Glc	7	25.4 ± 3.2	24.6
Galβ1,4Fruc	11	30.3 ± 4.1	24.6
Galβ1,4GlcNAc	6	30.9 ± 1.4	27.4
Galβ1,4Man	7	36.0 ± 2.4	24.4
Galβ1,3Ara	7	40.3 ± 3.3	23.5
Galβ1S1βGal	7	42.2 ± 3.3	25.2

[a] Calculated using differences in the solvent-accessible surface area as described in ref 15.

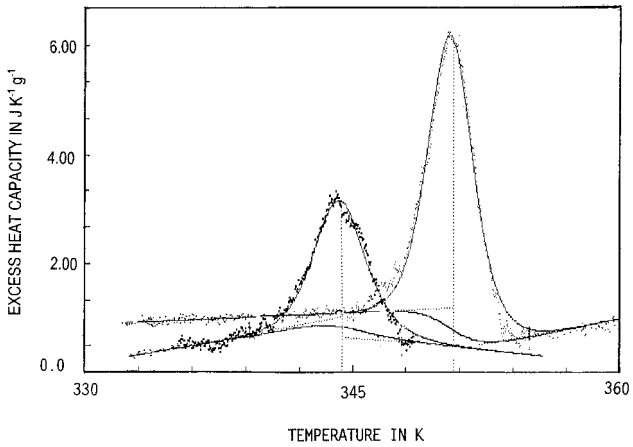

FIGURE 5: DSC scan of a 0.5 g sample of 0.043 mM galectin in PBS + 2 mM DTT and of a 0.5 g sample of 0.043 mM galectin in the presence of 7.7 mM MeO-2Galβ1,4Glc in PBS + 2 mM PBS (higher temperature peak) at a scan rate of 15 K h^{-1}. The solid lines are the best least-squares fits of the DSC data to the A ↔ B two-state transition model. The extrapolated baselines are also shown for the fits in addition to the vertical lines which show the location of T_m and T_l.

galectin is complexed with the ligand, it exists as a dimer at the denaturation temperature. The increase in T_l with increase in ligand concentration arises from preferential binding of the ligand to the lectin in the folded form. The denaturation of galectin in the presence of bound ligand can be expressed as (*30*)

$$AL_m = B + mL \tag{8}$$

and at constant lectin concentration

$$\ln [L] = -\Delta H_v(L)/\{mRT_l\} + \text{constant} \tag{9}$$

A typical plot of ln [L] versus $1/T_l$ is shown in Figure 6 for MeO-2Galβ1,4Glc. The best linear least-squares fits of ln [L] to $1/T_l$ for the carbohydrates yield values of $\Delta H_v(L)$ close to ΔH_v for $m = 2$ as shown in Table 6. Thus, one carbohydrate ligand binds to one monomer unit of galectin. This also supports the implication, from $\Delta H_c/\Delta H_v = 0.5-1.0$, that the galectin−carbohydrate complex exists as a dimer at the denaturation temperature; otherwise a larger value of m would be needed to satisfy the equality between $\Delta H_v(L)$ and ΔH_v from the peak shape. Determination of the binding constant from the DSC results and eq 6 at the denaturation temperature, K_b(DSC), shows agreement to within 30% with the extrapolated binding constant from the ITC measurements using eq 7 for Galβ1,4Glc, Galβ1,4Man, and Galβ1S1βGal. Values of K_b(DSC) for MeO-2Galβ1,4Glc are lower by at least a factor of 2 than those from extrapolation of the ITC results. This implies that this ligand may also bind slightly to the unfolded state of galectin; otherwise there would be more of a temperature increase with ligand concentration and, thus, better agreement with the ITC results.

DISCUSSION

The high specificity of carbohydrate−lectin interactions is evident in the X-ray crystallographic structure of the galectin−Galβ1,4GlcNAc complex. Not only does the shape of the binding pocket complement the galactopyranoside moiety of Galβ1,4GlcNAc but the electrostatic interaction of its axial 4′-OH with the N_η of Arg48 and an N_e of His44 of the galectin binding site is responsible for the specifically of the galectin for the galactopyranoside (*12*). In the X-ray crystallographic structure, the glucopyranoside moiety of the disaccharide exhibits possible hydrogen-bonding interactions between the acetyl group on C-2 and the side chains of Arg73 and Asp54 and the carbonyl of His52 mediated by a water

Table 5: Thermodynamic Quantities on the Thermal Denaturation of Galectin from DSC Measurements[a]

concn (mM)	T_m (K)	ΔH_v (kJ mol^{-1})	ΔH_c (kJ mol^{-1})	$\Delta H_c/\Delta H_v$
	Scan Rate = 15 K h^{-1} and pH = 7.6			
0.043−0.179	344.4 ± 0.8	956 ± 219	215 ± 9	0.22 ± 0.05
	Scan Rate = 25 K h^{-1} and pH = 7.6			
0.043−0.089	345.5 ± 0.5	958 ± 80	248 ± 25	0.26 ± 0.03
	Scan Rate = 15 K h^{-1} and pH = 6.8			
0.044	345.5 ± 0.2	1013 ± 73	342 ± 57	0.33 ± 0.06

[a] The calorimetric enthalpy, ΔH_c, is in units of kilojoules per mole of the galectin dimer (M_r = 28 000).

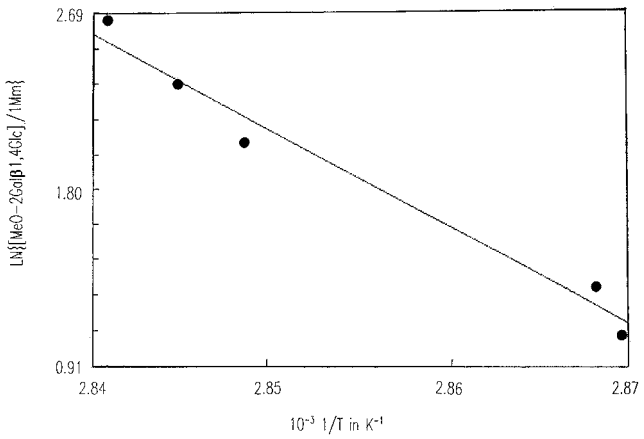

FIGURE 6: Plot of ln[ligand concentration] vs $1/T_l$ for MeO-2Galβ1,-4Glc. The line is the best linear least-squares fit of ln{[L]} to $1/T_l$.

molecule and between the C-3 OH group and Arg73, Arg48, and Glu71. Since modification of the glucopyranoside moiety alters the binding thermodynamics of the disaccharide for galectin (Table 1), they must involve changes in the interactions between the amino acid residues at the binding site and the groups on C-2 and C-3 of the glucopyranoside.

In relating changes in the binding thermodynamics of binding to the molecular interactions between the substituted glucopyranoside moiety and galectin, the binding enthalpies are compared since enthalpy−entropy compensation minimizes changes in $\Delta G_b°$ and changes in ΔH_b more accurately reflect changes in the carbohydrate−amino acid interactions of the complex (*31*). Comparison of the binding enthalpies to the structural interactions observed in the crystal complex are predicated on the assumption that the disaccharides being compared have the same solvation energy in water. With the exception of the MeO-2Galβ1,4Glc derivative, differences in the solvation energy of the disaccharide would arise from differences in the solvation energies of the substituted glucopyranoside moieties since the galactopyranoside moiety remains the same.

The binding enthalpies of Galβ1,4Man (−36.0 ± 2.4 kJ mol^{-1}), Galβ1,3Ara (−40.3 ± 5.5 kJ mol^{-1}), and Galβ1S1βGal(−42.0 ± 3.6 kJ mol^{-1}) are almost 20 kJ mol^{-1} more negative than the binding enthalpies of Galβ1,4Glc (−25.4 ± 3.2 kJ mol^{-1}) and Galβ1,3GlcNAc (−25.7 ± 2.5 kJ mol^{-1}), while the other disaccharides are all close to −30 kJ mol^{-1}. As with the Galβ1,4GlcNAc derivative, the lowest energy configuration of the glucopyranoside-substituted moiety for these disaccharides is the chair form as shown in Figure 3 so any difference in the binding enthalpies would involve the number and type of contacts formed between the substituted glucopyranoside moiety and the galectin binding site. Attempts to correlate the number of close contacts with the binding enthalpies were unsuccessful as shown in Table 4.

The binding enthalpies calculated from the change in the solvent-accessible surface area at the galectin binding site in Table 4, however, exhibit closer agreement with the experimental values for the binding enthalpies greater than −30.9 kJ mol^{-1}. The agreement in this table is poorer than that found when the same parameters are used in systems involving protein−peptide and protein folding interactions (*21*, *32*). It is clear that the calculations are able to model some general characteristics of the interactions between the disaccharides and the galectin binding site but fail to incorporate more detailed characteristics that lead to tighter binding for some of the sugars. It appears that a more complete model should include, in addition to the averaged terms represented by the buried surface area, terms that reflect the type of interactions such as the strength of the hydrogen bonds and polar/nonpolar interactions.

The approximate correlation of the binding enthalpy with the calculated binding enthalpy of the energy-minimized conformations for most of the disaccharides shows that the method based on changes in the solvent-accessible surface area can predict the binding enthalpies from the energy-minimized conformation of the complex derived from just one of the known crystal structures of the complex, the Galβ1,4GlcNAc−galectin complex. The determinants of the thermodynamic binding specificity for the glucopyranoside moiety are groups on C-2 and C-3 for the 1,4Glc moiety and hydroxy groups on C-4 and C-6 for the 1,3Glc moiety. For the other pyranoside rings, groups on C-1 also contribute to the thermodynamic binding specificity.

There is little effect of the methoxy group substituted for OH groups in Galβ1,4Glcβ-OMe and MeO-2Galβ1,4Glc on the binding enthalpy of Galβ1,4Glc using the criterion that binding enthalpies within two standard deviations are the same. In Galβ1,4Glcβ-OMe, the methoxy group is substituted for the C-1 OH group which plays little role in the binding interactions as evident by the absence of any

Table 6: Thermodynamic Quantities from DSC Measurements on the Thermal Transition of Galectin in the Presence of Ligands in PBS + 2 mM DTT Buffer[a]

ligand	ligand concn (mM)	T_m (K)	ΔH_v (kJ mol^{-1})	ΔH_c[b] (kJ mol^{-1})	$\Delta H_c/\Delta H_v$	ΔH(L)	K_b(DSC)/K_b[c]
Galβ1,4Glc	10−43	350.6−355.1	889 ± 56	781 ± 25	0.88 ± 0.09	930 ± 14	(759 ± 23)/1260
Galβ1,4Man	8−29	350.3−352.5	1038 ± 183	500 ± 90	0.48 ± 0.08	1110 ± 366	(591 ± 208)/867
MeO-2Galβ1,4Glc	3−14	348.1−351.8	964 ± 231	575 ± 90	0.60 ± 0.14	795 ± 71	(1192 ± 89)/3250
Galβ1S1βGal	4−27	348.4−353.7	1090 ± 7	700 ± 125	0.64 ± 0.11	1038 ± 56	(1144 ± 46)/837

[a] The uncertainties are standard deviations of the average values. [b] The calorimetric enthalpy, ΔH_c, is in units of kilojoules per mole of the galectin dimer (M_r = 28 000). [c] K_b(DSC) was determined from eq 5 in the text using T_m = 343.6 K and the upper values of ΔH_c for the first three ligands in the table.

interactions between the C-1 OH group and the amino acid residues at the binding site in the X-ray structure of the galectin−Galβ1,4GlcNAc complex (*12*). The upper limit binding enthalpy of −25.3 kJ mol^{-1} for MeO-2Galβ1,4Glc is the same as the binding enthalpy of Galβ1,4Glc (−25.4 ± 3.2 kJ mol^{-1}), and indeed, there is no identifiable interaction between the C-2 OH group on the galactopyranoside and the amino acid residues at the binding site in the X-ray structure (*12*). These latter two binding reactions further confirm using the known X-ray crystal structure of the galectin−Galβ1,4GlcNAc complex (*12*) as a starting structure to determine the close contacts between the disaccharide and galectin.

The enthalpically driven nature of the binding reaction and the enthalpy−entropy compensation mimic the binding properties observed for other lectins. Enthalpy−entropy compensation has been interpreted (*33*) to mean that as the ligand becomes more tightly bound to the protein (i.e., larger decrease in ΔH_b), its rotational and vibrational degrees of freedom will become more restricted and, thus, the entropy will decrease. Another explanation (*34*) for enthalpy−entropy compensation can arise from the assumption that the protein is in equilibrium between two different states, $P_0 \leftrightarrow P_1$, and that the ligand binds to either state with different affinities to produce mixed P_0L and P_1L complexes. This coupling between the binding process and the transition between the two states results in enthalpy−entropy compensation. Since the observed heat capacity change upon carbohydrate binding is 0, the enthalpy change for the $P_0 \leftrightarrow P_1$ is close to 0.

The DSC results show that galectin exists as a tetramer at the denaturation temperature and does not dissociate upon denaturation. This further association at higher temperatures has also been observed in DSC studies on the unfolding of catabolite activator protein from *Escherichia coli*, which also exists as a dimer at room temperature (*35*). This behavior is quite distinct from that observed by the legume lectins, all of which dissociate to monomers or submonomer units upon denaturation (1, 2, 4). In galectin, the two β-sheets of the monomers extend continuously across the dimer interface (*12*), whereas in concanavalin A and pea lectin, only one β-sheet is continuous. In the legume lectin, *Erythrina corallodendron* lectin, the sheets of the two monomers are roughly perpendicular (*36*), and this lectin undergoes denaturation and dissociation at a lower temperature than concanavalin A (*25*). The continuity of two β-sheets across the dimer interface compared to only one β-sheet being continuous across the monomer interface of the legume lectins apparently stabilizes the galectin dimer so that it does not dissociate upon denaturation. Thermal denaturation occurs at about 20 K lower than that of concanavalin A but close to that of lentil lectin and can be accounted for by the reduced size of the galectin dimer (28 kDa) relative to the concanavalin A dimer (50 kDa). Although association of galectin at the denaturation temperature is reduced upon disaccharide binding, as indicated by the higher $\Delta H_c/\Delta H_v$ ratios, the dimer still does not dissociate upon denaturation. The approximate agreement between K_b extrapolated from the ITC-determined values at room temperature and the K_b(DSC) values determined around 350 K for Galβ1,4Glc, Galβ1,4Man, and Galβ1S1βGal shows that the association of the unligated galectin at the denaturation temperature has very little effect on the binding process. This agreement also shows that the heat capacity change for the binding reaction is negligible over this temperature range as was observed between the low temperature and room temperature ITC results. The lower K_b(DSC) value for 2-MeOGalβ1,4Glc shows that apparently there is some bonding to the unfolded state which may occur through hydrophobic interactions between the hydrophobic core of the unfolded state.

REFERENCES

1. Schwarz, F. P., Puri, K., and Surolia, A. (1991) *J. Biol. Chem. 266*, 24344−24350.
2. Schwarz, F. P., Puri, K., Bhat, R. G., and Surolia, A. (1993) *J. Biol. Chem. 268*, 7668−7677.
3. Williams, B. A., Chervenak, M. C., and Toone, E. J. (1992) *J. Biol. Chem. 267*, 22907−22911.
4. Gupta, D., Dam, T. K., Oscarson, S., and Brewer, C. F. (1997) *J. Biol. Chem. 272*, 6388−6392.
5. Ramkumar, R., Surolia, A., and Podder, S. K. (1995) *Biochem. J. 308*, 237−241.
6. Drickamer, K. (1988) *J. Biol. Chem. 263*, 9557−9560.
7. Hirabayashi, J., and Kasai, K. (1993) *Glycobiology 3*, 297−304.
8. Barondes, S. H., Cooper, D. N. W., Gitt, M. A., and Leffler, H. (1994) *J. Biol. Chem. 269*, 20807−20810.
9. Leffler, H., and Barondes, S. H. (1986) *J. Biol. Chem. 261*, 10119−10126.
10. Sparrow, C. P., Leffler, H., and Barondes, S. H. (1987) *J. Biol. Chem. 262*, 7383−7390.
11. Ahmed, H., Allen, H. J., Sharma, A., and Matta, K. L. (1990) *Biochemistry 29*, 5315−5319.
12. Liao, D., Kapadia, G., Ahmed, H., Vasta, G. R., and Herzberg, O. (1994) *Proc. Natl. Acad. Sci. U.S.A. 91*, 1428−1432.
13. Leffler, H., and Barondes, S. H. (1986) *J. Biol. Chem. 261*, 10119−10126.
14. Lee, R. T., Ichikawa, Y., Allen, H. J., and Lee, Y. C. (1990) *J. Biol. Chem. 265*, 7864−7871.
15. Luque, I., Mayorga, O. L., and Freire, E. (1996) *Biochemistry 35*, 13681−13688.
16. Ahmed, H., Fink, N. E., Pohl, J., and Vasta, G. R. (1996) *J. Biochem. (Tokyo) 120*, 1007−1019.
17. Wiseman, T., Williston, S., Brandts, J. F., and Lin, L. N. (1989) *Anal. Biochem. 179*, 131−137.
18. Yang, C. P. (1990) *Omega Data in Origin*, p 66, Microcal Inc., Northhampton, MA.
19. Evans, S. V. (1993) *J. Mol. Graphics 11*, 134−138.
20. Bianchet, M. A., Ahmed, H., Vasta, G. R., and Amzel, L. M., private communication.
21. Murphy, K. P., Xie, D., Garcia, K. C., Amzel, L. M., and Freire, E. (1993) *Proteins 15*, 113−120.
22. Collaborative Computional Project No. (1994) The CCP4 Suite: Programs for Protein Crystallography, *Acta Crystallogr. D 50*, 760−763.
23. Lee, B., and Richards, F. M. (1971) *J. Mol. Biol. 55*, 374−400.
24. Kirchhoff, W. H. (1993) Exam: A Two-State Thermodynamic Analysis Program, NIST Technical Note 1401, 1−103.
25. Surolia, A., Schwarz, F. P., and Sharon, N. (1996) *J. Biol. Chem. 271*, 17697−17703.
26. Ahmed, H., Pohl, J., Fink, N. E., Strobel, F., and Vasta, G. R. (1996) *J. Biol. Chem. 271*, 33083−33094.
27. Ahmed, H., and Vasta, G. R. (1994) *Glycobiology 4*, 545−549.
28. Sanchez-Ruiz, J. M., Lopez-Lacomba, J. L., Cortijo, M., and Mateo, P. L. (1988) *Biochemistry 27*, 1648−1652.
29. Manly, S. P., Matthews, K. S., and Sturtevant, J. M. (1985) *Biochemistry 24*, 3842−3846.
30. Fukada, H., Sturtevant, J. M., and Quiocho, F. A. (1983) *J. Biol. Chem. 258*, 13193−13198.

31. Brown, J., and Schwarz, F. P. (1997) *Carbohydr. Res.* (submitted for publication).
32. Hilser, V. J., Gomez, J., and Freire, E. (1993) *Proteins 26*, 123−133.
33. Leffler, J. E., and Grunwald, E. (1963) *Rates and Equilibria of Organic Reactions*, pp 315−402, John Wiley and Sons, Inc., New York.
34. Eftink, M. R., Anusiem, A. C., and Biltonen, R. L. (1983) *Biochemistry 22*, 3884−3896.
35. Ghosaini, L. R., Brown, A. M., and Sturtevant, J. M. (1988) *Biochemistry 27*, 5258−5261.
36. Shaanan, B., Lis, H., and Sharon, N. (1991) *Science 254*, 862−866.

BI9716478